RADIATION DAMAGE OF COMPONENTS IN THE ENVIRONMENT OF HIGH-POWER PROTON ACCELERATORS

D. Kiselev, R. Bergmann, R. Sobbia, V. Talanov, M. Wohlmuther,
Paul Scherrer Institut, 5232 Villigen, Switzerland

Abstract

At high power accelerators, radiation damage becomes an issue particularly for components which are hit directly by the beam, like targets and collimators. Protons and secondary particles change the microscopic (lattice) structure of the materials, which macroscopically affects physical and mechanical properties. Examples are the decrease of thermal conductivity and ductility as well as dimensional changes. However, the prediction of these damage effects and their evolution in this harsh environment is highly complex as they strongly depend on parameters such as the irradiation temperature of the material, and the energy and type of particle inducing the damage. The so-called term "displacements per atom" (DPA) is an attempt to quantify the amount of radiation induced damage and to compare the micro- and macroscopic effects of radiation damage caused by different particles at different energies.

In this report, the basics for understanding of the mechanisms of radiation damage will be explained. The definition and determination of DPA and its limitations will be discussed. Measurements and examples of the impact of radiation damage on accelerator components will be presented.

INTRODUCTION

The change in material properties due to damage to the lattice structure, which sometimes leads to the failure of components, is called radiation damage. It is a threat particularly to components at loss points in high-power accelerators. These components include targets, beam dumps, and highly exposed collimators. There is renewed interest in the topic of radiation damage owing to new projects and initiatives which require high-power accelerators, and therefore materials which will withstand high power sufficiently long. One such project is the European Spallation Source (ESS), which is being built in Lund, Sweden [1] with a rotating wheel target composed of tantalum cladded tungsten bars irradiated with 5 MW of 2.5 GeV protons. The Facility for Rare Ion Beams (FRIB) is being built at the National Superconducting Cyclotron Laboratory (NSCL) at Michigan State University. This facility will deliver heavy ions with extremely high power densities of 20–60 MW/cm^3 [2]. The Daedalus project is an initiative at MIT with the aim of studying CP violation [3]. For this purpose, a neutrino beam shall be produced by three cyclotrons, each delivering a proton beam with energy of about 800 MeV. The planned beam power on target are foreseen to be 1, 2, and 5 MW for the first, second, and third cyclotron, respectively. At PSI, a 1.3 MW proton beam is routinely available, which constitutes the most intense steady state proton source in the world at present. Higher powers of up to 1.8 MW are envisaged for the future.

For all these projects, it is essential to know how long the heavily irradiated components can be operated safely. In addition, improvement of the lifetime of components needs knowledge about the underlying mechanism of radiation damage and its relation to the changes in material properties. One problem is that components cannot be tested under the same conditions as experienced during operation. Therefore, the correlations between data obtained under different conditions need to be understood.

Prominent macroscopic effects on structural materials caused by radiation damage are the following:

- Hardening, which leads to a loss of ductility;
- Embrittlement, which leads to fast crack propagation;
- Growth and swelling, which lead to dimensional changes of components and can also induce additional mechanical stress;
- increased corrosion rates, in particular in contact with fluids;
- irradiation creep, which leads to deformation of components;
- Phase transformations in the material or segregation of alloying elements, which leads to changes in several mechanical and physical properties.

Besides changes of structural mechanical properties physical properties change as well. Particularly serious is the steep decrease of the thermal conductivity for components, which need to be heavily cooled due to the energy deposition of proton beams. Design studies rely on prediction of the temperature distribution in a component and thus on the knowledge of the thermal conductivity of the material. The consequence is that the component might reach higher temperatures than foreseen, which could lead to the failure of the component.

In pulsed sources, components in addition undergo thermal cycles, causing fatigue. Cracks may occur, which could lead to failure of the component. This phenomenon might be also influenced and accelerated by radiation due to additional hardening and embrittlement. Sometimes, a phenomenon attributed to radiation damage, might in fact be caused by other effects like e.g. rapid heating or pitting.

In the following, some examples of observed radiation damage will be given. In preparation for the above-mentioned FRIB, several objects were studied at NSCL with respect to radiation damage due to heavy ions. For this purpose, a 580 mg/cm^2 tungsten foil, which corresponds to a thickness of 0.03 cm, was irradiated with 76Ge30+ ions at 130 MeV/nucleon. After irradiation of

Copyright © 2016 CC-BY-3.0 and by the respective authors

ISBN 978-3-95450-167-0

the tungsten foil with 5.77×10^{16} Ge ions on a beam spot with diameter of 0.6–0.8 mm, a crack was observed right in the centre of the beam spot. Further investigations [2] revealed that the crack was caused by swelling and embrittlement, which induced additional stress in the foil. Due to the likely decrease of the thermal conductivity by radiation the stress might have been increased by thermal stress.

At the Los Alamos National Laboratory, tungsten was investigated for its suitability as a material for spallation targets. For this, hardness and compression tests were performed at room temperature and at 475°C on irradiated and un-irradiated specimens. Tungsten rods were irradiated for up to 6 months with 800 MeV protons at a current of 1 mA, which corresponds to a dose of 23 Displacements Per Atom (DPA). The temperature during irradiation was kept constant for each sample; it varied between 50 and 270°C for different samples. In the compression tests, the samples were compressed to a strain of about 20%. The irradiated samples suffered from a loss of ductility, which showed up as a longitudinal crack in the compression tests, i.e. in the direction of the force. The compressive yield stress and the hardness increased linearly with the dose except for small doses, where it increased strongly. Optical micrographs of the tungsten compression specimens were also taken [4].

The pyrolytic graphite target at TRIUMF was cooled on the edges with water. After irradiation with 500 MeV protons at a current of 120 μA, the graphite delaminated, i.e. segmented into slices perpendicular to the beam. It is interesting to note that the target stayed intact for currents below 100 μA, however always failed at higher currents. For details and a picture of the target after irradiation, see Ref. 5. After improving the cooling swelling was not observed anymore [6]. This agrees with the assumption that swelling is a high temperature effect. A similar phenomenon was observed at PSI, where a former meson production target made from Beryllium always cracked at 150 μA, but survived at smaller currents. This might be a hint that the damage was influenced also by thermal stress.

At the 1 MW spallation source at SNS examination of the irradiated container of the mercury target revealed an interesting damage pattern, which is not correlated with the beam intensity. Fluid dynamic simulations could show that the damage is correlated with the flow distribution of the mercury. Finally, the damage was attributed to thermal shock caused by the beam in the mercury, which leads to cavitation and pitting on the stainless steel container [7].

UNDERLYING MECHANISM OF RADIATION DAMAGE

When particles penetrate matter they lose energy by several different mechanisms, where some of them will damage the lattice structure of the material. The mechanisms are:

- electronic excitations/ionisation;
- elastic interactions;
- inelastic reactions.

The first of these types of interaction is due to the Coulomb interaction and is therefore possible only for charged particles. Here, energy is used to shift electrons from the atomic core to an outer shell. This is called excitation and can lead to the removal of an electron, i.e. ionization of the atom. The excess energy is dissipated as heat, which might also cause damage to structural materials like a copper beam dump, although this kind of damage has nothing to do with radiation damage. However, in organic materials ionization causes damage by breaking bonds. Therefore, plastics or grease become dark, hard and brittle. The damage due to ionisation is quantified by the ionising dose, which is the absorbed dose in the material (unit Gray). This is a cumulative effect over time. The method to calculate the absorbed dose is well known.

In elastic and inelastic interactions, energy and momentum are transferred from the particle to the nucleus. In case of an elastic interaction, the nucleus is not changed but remains the same isotope. In all cases, the atom gains a recoil momentum. The first atom hit is called the Primary Knocked-on Atom (PKA). Energy and momentum are transferred to the nucleus only and not to its electrons; hence the atom moves in a partly ionized state through the lattice. The recoil energy is mainly lost mainly by Coulomb interactions (ionization and excitation) and is again dissipated as heat. If the energy is large enough, the primary atom can knock on other atoms, which again leave their site. As a result, many atoms can be moved from their original lattice position.

The inelastic reaction usually transfers a larger portion of energy to the atom compared to elastic interactions. Inelastic interactions lead to transmutation of the nucleus, which can be radioactive, but also to the production of many secondary particles. The transmuted nucleus, referred to as an impurity in the following, does not fit ideally into the lattice structure and therefore changes the mechanical properties of the material. Furthermore, in high-conductivity materials such as very pure copper, impurities are known to reduce the conductivity, i.e. they also have an influence on the physical properties. Usually, the damage done to the lattice by the recoils is much larger than that due to the impurities. An exception is when large amounts of helium and hydrogen are produced in highly energetic reactions..

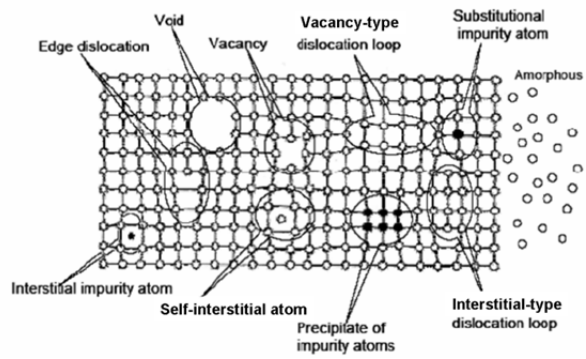

Figure 1: The most important defects in a lattice structure (image from Prof. H. Föll, University of Kiel).

ISBN 978-3-95450-167-0

Copyright © 2016 CC-BY-3.0 and by the respective authors

The most important defects in a lattice are shown in Fig. 1. The open dots belong to the original crystal, and the black dots indicate impurities. The simplest defects are the point defects, also known as zero-dimensional defects. The most prominent representatives of the point defects are self-interstitials and vacancies. Self-interstitials are atoms from the lattice which have left their lattice position for a site not provided in the lattice. The influence of a self-interstitial on its surroundings is a shift of neighbouring atoms away from the self-interstitial to make space for it. A vacancy is just the opposite of a self-interstitial. Here, a lattice atom is missing. These defects also exist in un-irradiated materials. If a defect of this type is caused by irradiation, a vacancy and a self-interstitial appear in a pair. This is called a Frenkel pair. Also, an atom on an interstitial site may have been transmuted by an inelastic reaction to an impurity. It is then called an interstitial impurity atom or extrinsic interstitial.

The dislocation loop belongs to the class of one-dimensional defects. Here, part of a lattice plane is missing or has been added. There are two types of dislocation loop: the vacancy-type dislocation loop and the interstitial-type dislocation loop. In the vacancy type, part of a plane of lattice sites is missing. In the interstitial type, part of a plane of additional atoms has been incorporated into the lattice structure. Dislocations move under the influence of external forces, which cause internal stresses in a crystal. In the ideal case, dislocations move out of the lattice. If more than one plane is involved, a cluster is formed. If several planes are partly missing, one has an agglomeration of vacancies. This is called a void. An agglomeration of impurity atoms replacing neighbouring lattice sites on more than one plane is called a precipitate. Owing to their different sizes and properties, the neighbouring atoms are slightly shifted from their original positions. All of these defects make the lattice less flexible against strain, which manifests in a loss of ductility and an increase in hardness. In addition, the material becomes brittle. Small cracks can develop, which may grow further, and this can lead to the failure of a component.

Usually, the interaction with a particle of more than a few MeV does not cause single defects of the kind described above; instead, a large region containing millions of atoms is affected. For example, a nucleus in gold with a recoil energy of only 10 keV destroys the lattice structure in its surroundings within a radius of about 5 nm. This is called a displacement spike and happens within 1 ps. Since a huge number of atoms is involved in the process, a simulation via a Monte Carlo technique needs considerable effort and a large amount of computer power. Such a simulation has to solve the equation of motion for all atoms at the same time, since each atom can interact with and be influenced by all the other atoms. This is a multibody problem, and the computer time needed grows with the square of the recoil energy of the first knock-on atom. The higher the recoil energy, the greater the number of atoms involved. Therefore such calculations are limited to recoil energies less than 100 keV for practical reasons. In addition, the simulation has to be repeated for each recoil energy. This kind of calculation is called Molecular Dynamics Simulation (MDS). The advantage is that the results are quite realistic, and the various kinds of defects produced can be studied in the simulation. The MDS method is the only way to evaluate how many defects disappear as a result of recombination with other defects. Unfortunately, the MDS method can follow the process for only a few picoseconds, whereas the complete healing process can last for months.

A faster but less accurate method is the Binary Collision Approximation (BCA), where only collisions between two (hence the name 'binary') atoms are considered. The other atoms are considered as spectators. The particles are followed via trajectories as in a Monte Carlo particle transport program. This calculation method is much faster than the MDS method and also works well at higher energies. However, when such approximations are made, much less information about the process and the state of the lattice is available compared with the MDS method.

CALCULATION OF DPA

To estimate and quantify the severity of the damage, a phenomenological approach was developed by Norgett, Robinson, and Torrens, which dates back to the 1970s [8], known as the NRT model after the authors' initials. To quantify the radiation damage, a value is chosen which indicates how often each atom is displaced on average during the irradiation. This quantity is called the Displacement Per Atom (DPA), and is obtained by convolution of the energy-dependent particle fluence $\phi(E)$ (in units of particles/cm^{-2}) with the displacement cross-section $\sigma_{\mathrm{disp}}(E)$:

$$DPA = \int \sigma_{\mathrm{disp}}(E)\ \frac{\mathrm{d}\phi(E)}{\mathrm{d}E}\ \mathrm{dE} \qquad (1)$$

The displacement cross-section gives the number of displacements per particle. It is a function of the energy of the particle responsible for the damage. For charged particles the displacement cross section is determined by the Coulomb interaction at low energy and therefore large, for ions even larger than for protons. Above 10 MeV the displacement cross section is dominated by nuclear reactions and the production of secondary particles and their interactions. Therefore, at higher energies the displacement cross section of protons and neutrons is very similar.

The displacement cross-section is obtained by folding the damage cross section with the damage function $\nu(E_{\mathrm{R}})$ described below:

$$\sigma_{\mathrm{disp}}(E) = \int_{E_{\mathrm{D}}}^{E\,\mathrm{max}} \frac{\mathrm{d}\sigma_{\mathrm{dam}}(E, E_{\mathrm{R}})}{\mathrm{d}E_{\mathrm{R}}}\ \nu(E_{\mathrm{R}})\ \mathrm{d}E_{\mathrm{R}} \qquad (2)$$

The integration runs over all recoil energies from the threshold, i.e. E_{D}, to the maximum possible recoil energy. The damage cross-section $\sigma_{\mathrm{dam}}(E, E_{\mathrm{R}})$ is, in addition, a function of the recoil energy of the PKA and is in fact calculated from the recoil spectrum $w(E_R)$. It states how

Copyright © 2016 CC-BY-3.0 and by the respective authors

ISBN 978-3-95450-167-0

many nuclei can be found with recoil energy E_R. It is obtained from

$$\frac{d\sigma_{dam}(E,E_R)}{dE_R} = \frac{dw(E,E_R)/dE_R}{xN_V}, \quad (3)$$

where x is the thickness of the sample and N_V is the atom density in atoms/cm^3. To obtain the recoil spectrum, the cross-sections of all reactions occurring in the material have to be known. Since Monte Carlo particle transport programs contain models for all nuclear reaction cross-sections over a wide energy range, a popular application of these programs is to use them to obtain the recoil spectrum. Here, it is important to use a thin target to avoid significant energy loss of the primary particle in the sample. If the object of interest has larger dimensions, the recoil spectrum has to be calculated for different energies of the primary particle to account for the energy loss of that particle. This requires several Monte Carlo runs. Besides this the fluence required in Eq. (1) is calculated in Monte-Carlo particle transport programs. Many such codes like FLUKA, PHITS, and MARS already have a built-in option to obtain the DPA in one run. This is very convenient and avoids a larger effort. Alternatively, one can use Eq. (1) folding the calculated fluence with displacement cross sections provided somewhere else. Eq. (1) has to be applied not only for the primary particle but also for the secondary particles produced.

The energy available to displace other atoms is called the damage energy, T_{dam}, which is equal to the recoil energy minus the energy E_e dissipated in ionization and excitation of the atom. For recoil energies larger than 10 keV, most of the energy is lost by ionization. The fraction of the recoil energy left for the damage energy is called the partition function or, sometimes, the damage efficiency. The amount of energy required for displacing an atom is roughly twice the sublimation energy because, at the surface, only half of the bonding needs to be broken. In Cu, the energy needed ranges from 18 to 43 eV, depending on the crystal orientation [9]. In most calculations, the effective threshold energy E_D for copper is taken equal to 30 eV. When the damage energy T_{dam} is larger than E_D but less than $2E_D$, just one atom can be displaced. The PKA may be captured on the lattice site of the second atom. Since for $E_R = 2E_D$ only one atom is effectively displaced, the damage function $\nu(E_R)$, which gives the number of displaced atoms, is given by

$$\nu(E_R) = \frac{\kappa T_{dam}}{2E_D}$$

The factor κ is set to 0.8, which was obtained by a BCA calculation of the authors of [8]. For $E_R > 2E_D$, a cascade of collisions and displacements will take place.

It has to be emphasized that the NRT approach is a simplified method. It completely neglects the details of the process of the displacement cascade. No interactions of the struck atom with the remaining lattice atoms are taken into account. Parameters of the crystal lattice such as the atomic bonding energy and the properties of the solid are completely absent. Instead, all this is condensed into the displacement threshold energy E_D. In the NRT model, it is implicitly assumed that the defect concentration is equal to the calculated number of displacements. Moreover, the displacements formed are taken to be stable. Molecular dynamics simulations have shown that the defects are not isolated Frenkel pairs as assumed in the NRT model, but are concentrated in a small region influencing each other. A high density of displaced atoms is produced in the first few tenths of a picosecond. This is called the collisional phase. In this phase, the number of displaced atoms is in fact much larger than that predicted by the NRT model. A few picoseconds later, most of the displaced atoms have recombined with vacancies. This is called 'healing'. The interstitial–vacancy annihilation process is completely omitted in the NRT model. This process is especially important at large PKA energies (>5 keV), where cascades of displaced atoms are produced in the initial state and defects are produced close to each other. At higher PKA energies (>20 keV), subcascades are formed and the number of recombination events decreases. Such a high-energy atom shakes the whole lattice and also deposits thermal energy, localized in the defect region. E.g., 10 keV recoil on gold produces a displacement spike with an equivalent temperature of 10000 K. This makes the defects more mobile and facilitates recombination. The assumption of the NRT model that it is sufficient to count the initially produced Frenkel pairs cannot be justified at energies larger than 0.5 keV, where high-energy cascades start to develop.

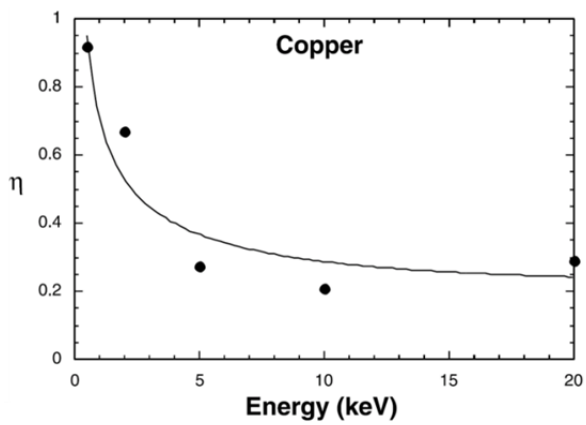

Figure 2: Defect efficiency as a function of the recoil energy in copper [10] at 4 K.

An example of the effect of healing in copper is shown in Fig. 2. The effective healing is just $1 - \eta$, where η is the defect or cascade efficiency. It is given as a function of the recoil energy of the PKA. The defect efficiency η is defined as the ratio of the number of Frenkel pairs at the end of phase 1, i.e. at the end of the collision cascade, obtained by an MDS, to the number obtained from the NRT model [10]. The MDS calculation here was performed for a temperature of 4 K. The results confirm that

ISBN 978-3-95450-167-0

Copyright © 2016 CC-BY-3.0 and by the respective authors

the NRT approach is only justified at small recoil energies. Above 5 keV the recombination of defects dominates. The number of Frenkel pairs is five times lower than predicted by the NRT model. This kind of healing is called athermal as it is independent of the temperature and takes place within 50 ps. It is interesting to note that the defect efficiencies in other materials such as W, Fe, and Al show very similar values, even though the final distribution of the defects differ.

Another healing effect is causes by external temperature and therefore also called thermal healing. Already low temperatures (>10 K) make the atoms sufficiently mobile to recombine with vacancies. This effect takes places on a much longer time scale of hours to years – depending on the temperature. It is well known that due to annealing after irradiation the properties of the material are getting closer to the ones of the unirradiated state. In Fig. 3 the surviving defect fraction is shown as a function of temperature for copper.

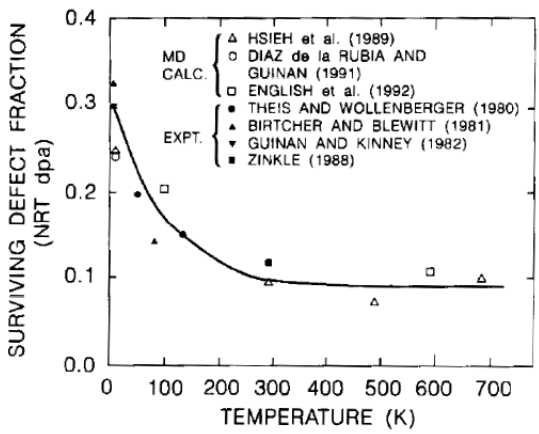

Figure 3: Thermal healing: Surviving defect fraction as a function of temperature for copper [11].

The reduction of the defect efficiency at high PKA energy is important when one is comparing the damage produced by low- and high-energy particles. The materials that suffer radiation damage at today's accelerators are irradiated by high-energy particles, whereas most of the material studies were done in reactors. Figure 2 suggests that one has just to multiply the recoil spectrum of the PKA by the defect efficiency to compare the results and to profit from the large data set that has been taken with reactor neutrons. However, the effect of irradiation can depend on many details, e.g. the production of impurities, specially hydrogen and helium (see below). The good news is that the NRT–DPA method provides a conservative value for DPA.

MEASUREMENT OF DEFECTS

Although the NRT-DPA cannot be measured directly since most of the defects heal out within 50 ps, the number of final defects can be determined by several methods. The increase of the electrical resistivity is directly related to the number of Frenkel pairs created times the contribution to the electric resistivity of one Frenkel pair. The latter quantity is known from X-ray scattering. Comparison of experimental data with MDS revealed satisfying agreement [10]. The defect production efficiency can be obtained by comparing the measured defects with the one predicted by NRT as shown in Fig. 3. However, defects do not consist solely of Frenkel pairs but also of e.g. clusters. It turns out that in most metals clusters contribute with a similar resistivity as Frenkel pairs. In addition, such experiments are usually done at very low DPA, where single defects like Frenkel pairs dominate.

Defects can be also visualized. A common method is using the Transmission Electron Microscope (TEM), which requires very thin samples to detect the transmitted electrons on the backside of the sample. Nowadays resolutions of a few nm are possible. In addition, even in situ TEM just after the irradiation and a few seconds later were performed [12], which revealed the disappearance of nanovoids. However, only defects above the resolution are visible. In addition, the defect distribution measured on materials irradiated at different temperatures and DPA can look very different. Counting the number of defect clusters shows a clear disappearance of defects with temperature, however, the number of single point defects increases. Further, the saturation of the number of defects after a few DPA in stainless steel 316L was measured in a similar way [13] and is valid also for other materials.

TENSION TESTS AND HELIUM

Although different kinds of post irradiation experiments are performed, one common measurement is the tension test, where the material is pulled at both ends until its rupture. Irradiated samples are in general harder, i.e. the tensile strength is higher than in the unirradiated case. In addition, the material becomes more brittle, which can be also seen from the strain-stress diagram. A break of the sample without necking is a clear sign for embrittlement. At high temperatures the embrittlement can be even accelerated by helium produced by inelastic reactions (mostly spallation). Some materials like austenitic steel are really sensitive and a few appm He is sufficient for He induced embrittlement at higher temperature.

Since the hydrogen and helium production can influence the mechanical properties it is important always to note to which H/He content and at which temperature the material was irradiated. The production of He at high energy accelerators can exceed that in fission reactors by about a factor of 100, when high energy particles hit the component directly. Hydrogen production can be increased by a factor 400 to 500 in accelerators compared to fission reactors. Therefore, the large database of measurements in reactors has to be used with care to predict radiation damage at accelerators. Hydrogen leaves e.g. steels at temperatures larger than 250 °C. In metals, which form hydrids, hydrogen leads to embrittlement at lower temperature.

Copyright © 2016 CC-BY-3.0 and by the respective authors

ISBN 978-3-95450-167-0

Helium bubbles can be well visualized with the already mentioned TEM method. They appear as small dots/bubbles equally distributed over the sample. Besides the embrittlement He influences the swelling although both effects, accelerating and reducing swelling, were observed. Another interesting and well visible effect is the blistering or exfoliation of small pieces on the surface. The pressure between larger bubbles just below the surface causes stress, which is not balanced by the tension stress at the surface. Therefore fractures on the surface occur. Such an effect was observed in experiments using He beams. Due to its short range He is implanted just below the surface where it forms bubbles.

INSPECTION OF A COLLIMATOR AT PSI

The collimator KHE2 is located 4.5 m behind the meson production target E, a 4 cm thick graphite wheel, in the 590 MeV proton beam line. Due to multiple scattering the beam is spread in addition to its intrinsic divergence by 6 mrad. To shape the beam the KHE2 absorbs about 10 % of the beam on Target E, i.e. it suffers from a power deposition of about 130 kW. Therefore, it consists of a copper body, 30 cm long (proton stopping range in Cu is 26 cm), and brazed steel tubes around for cooling with water. The KHE2 was in operation from 1990 until 2012. In this period the beam on Target E increased steadily; the integrated charge was 147 Ah. ANSYS calculations using the thermal conductivity of unirradiated copper show a maximum temperature of 380°C inside the collimator at 2 mA. The first 5 cm long section of the inner part of KHE2 experiences an average of 30 DPA, the outer part 4 DPA according to a calculation with MARS [14]. Although MCNPX2.5.0 [15] predicts half of the values obtained with MARS, measurements at similar temperature but performed in reactors, suggested a swelling rate of 0.5 %/DPA. Therefore, the collimator was taken out of the beam line and inspected with a well shielded camera and two laser distance meters for measuring the opening of the collimator. The horizontal dimensions of the apertures of the six "teeth" were measured with the two laser distance meters and a prism mirror. The original values could be reproduced by the measurement with a deviation of less than 0.2 mm, where 0.5 mm corresponds to the accuracy of the method. Another proof of the absence of a dimensional change due to swelling is the slit of 1 mm for thermal expansion, which is completely intact at the entry as well as at the exit side of KHE2.

In Fig. 4, a view of the front of the collimator is shown. In the vertical and horizontal direction, erosion/blistering of the surface can be seen around the slits, which help to release thermal stress. Most astonishing the surface between the horizontal and vertical view is much less affected, although the beam profile is almost circular. A possible explanation might be that around the slits there is more movement of the surfaces due to thermal expansion and shrinking when the beam is on or off. The blistering might be partly due to the helium deposition close to the surface. Between the horizontal and vertical direction, a grey film appears on the surface, which is probably graphite evaporated from Target E. A sample containing Be7 confirms this. On the right of Fig. 4, photos of the vertical surfaces at the beam exit and the horizontal surface at the beam entry are seen. Although the temperature of about 80 to 100 °C does not vary much throughout the collimator at the vertical position, the surface at the beam exit (top picture on Fig. 4) looks much more eroded than at the entry. Pieces of the grey surface are 1-2 mm high and are peeling off. The surfaces at the top and the bottom look essentially the same.

Figure 4: Left: Collimator front view with Ni-aperture. Right: Photo from the exit, vertical position, and entry at horizontal position (picture on the bottom).

At the horizontal surfaces the grey coating cannot be seen, most likely because this is the hottest surface. However, exfoliation also appears here and it seems that some lamella took already off.

REFERENCES

[1] European Spallation Source, http://ess-scandinavia.eu
[2] R. Ronningen, in *Proc. HB2010*, Morschach, Switzerland, Sept. 2010, pp. 662-666.
[3] J.M. Conrad *et al.*, arXiv:1012.4853 [hep-ex].
[4] S.A. Maloy *et al.*, *J. Nucl. Mater.,* vol. 34, p. 219, 2005.
[5] E.W. Blackmore *et al.*, in *Proc. PAC 2005*, Knoxville, USA, May 2005, pp. 1919-1921.
[6] E.W. Blackmore, private communication.
[7] B. Riemer *et al.*, *J. Nucl. Mater.*, vol. 450, p. 183, 2014.
[8] M. Norgett, M. Robinson, and I. Torrens, *Nucl. Eng. Des.,* vol. 33, p. 50, 1975.
[9] H.B. Huntington, *Phys. Rev.,* vol. 93, p. 1414, 1954.
[10] M.J. Cartula *et al.*, *J. Nucl. Mater.*, vol. 296, p. 90, 2001.
[11] B.N. Singh, S. Zinkle et al, *J. Nucl. Mater.*, vol. 206, p. 212, 1993.
[12] Y. Chen *et al*, *Nat. Commun.* 6:7036 doi:10.1038/ncomms8036, 2015.
[13] D.J. Edwards, E.P. Simonen, S.M. Bruemmer, *J. Nuc. Matter.*, vol. 317, p. 13, 2003.
[14] N.V. Mokhov, S.I. Striganov, "MARS15 Overview", Fermilab, USA , Fermilab-Conf-07-008-AD, 2007.
[15] D. Pelowitz, ed., "*MCNPX User's Manual, Version* 2.5.0", Los Alamos, USA, Rep. LA-CP-05-0369, 2005.

ISBN 978-3-95450-167-0

Copyright © 2016 CC-BY-3.0 and by the respective authors